Journal of Hazardous Materials 434 (2022) 128906

Contents lists available at ScienceDirect

Journal of Hazardous Materials

journal homepage: www.elsevier.com/locate/jhazmat

Hazardous enrichment of toxic elements in soils and olives in the urban zone of Lavrio, Greece, a legacy, millennia-old silver/lead mining area and related health risk assessment

Vasileios Antoniadis [a], Giorgos Thalassinos [a], Efi Levizou [a], Jianxu Wang [b], Shan-Li Wang [c], Sabry M. Shaheen [d,e,f], Jörg Rinklebe [d,*,1]

[a] Department of Agriculture Crop Production and Rural Environment, University of Thessaly, Greece
[b] State Key Laboratory of Environmental Geochemistry, Institute of Geochemistry, Chinese Academy of Sciences, 550082 Guiyang, PR China
[c] Department of Agricultural Chemistry, National Taiwan University, No.1, Section 4, Roosevelt Road, Taipei 106 Taiwan
[d] University of Wuppertal, School of Architecture and Civil Engineering, Institute of Foundation Engineering, Water, and Waste-Management, Laboratory of Soil, and Groundwater-Management, Pauluskirchstraße 7, Wuppertal 42285, Germany
[e] King Abdulaziz University, Faculty of Meteorology, Environment, and Arid Land Agriculture, Department of Arid Land Agriculture, Jeddah 21589, Saudi Arabia
[f] University of Kafrelsheikh, Faculty of Agriculture, Department of Soil and Water Sciences, 33516 Kafr El-Sheikh, Egypt

HIGHLIGHTS

- Ag, As, Cd, Pb, Sb, and Zn were dramatically enriched in a millennia-old Ag/Pb mine.
- XANES analysis revealed that As was primarily associated with scorodite.
- Soil-to-plant transfer of Cd was high in *Malva sylvestris*.
- Olives surpassed the limits for Cd and Pb, thus, a consumption should be avoided.
- Cancer risk of As exposure was unacceptably high, well beyond the 1×10^{-4} threshold.

GRAPHICAL ABSTRACT

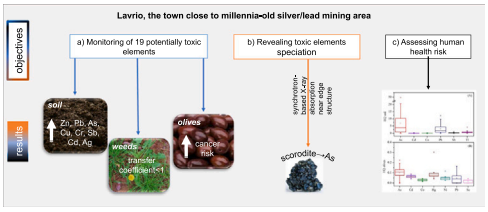

ARTICLE INFO

Ediotr: Lingxin CHEN

Keywords:
Hazardous metal(loids)
Carcinogenic risk
Non-carcinogenic risk
Table olives
Uptake by weeds

ABSTRACT

Lavrio is a Greek town with several abandoned Ag/Pb mines. In this study, 19 potentially toxic elements (PTEs) were measured in soil, weeds, and olives. Levels of seven of the studied PTEs in soil were highly elevated: Zn (56.2–58,726 mg kg^{-1}), Pb (36.2–31,332), As (7.3–10,886), Cu (8.3–1273), Sb (0.99–297.8), Cd (0.17–287.7), and Ag (0.09–38.7). Synchrotron-based X-ray absorption near edge structure analysis of the soils revealed that As was predominantly associated with scorodite, Pb with humic substances, Zn with illite, $Zn(OH)_2$ and humic substances, and Fe with goethite-like minerals. The transfer of the PTEs to weeds was relatively low, with the transfer coefficient being less than 1.0 for all PTEs. Cadmium in table olives surpassed 0.05 mg kg^{-1} fresh weight (the limit in EU), while Pb surpassed its limit in approximately half of the samples. Health risk assessment confirmed soil contamination in the study area where As and Pb hazard quotients were well above 1.0 and the average hazard index equaled 11.40. Additionally, the cancer risk values exceeding the 1×10^{-4} threshold. The results obtained in the study indicate that Lavrio urgently requires an adequate ecofriendly remediation plan,

* Corresponding author.
E-mail address: rinklebe@uni-wuppertal.de (J. Rinklebe).
[1] ORCiD: 0000-0001-7404-1639

https://doi.org/10.1016/j.jhazmat.2022.128906
Received 11 November 2021; Received in revised form 7 April 2022; Accepted 10 April 2022
Available online 14 April 2022

including revegetation with tolerant species and targeted efforts to chemically stabilize harmful PTEs. The presented approach may serve as a pivotal study for industrial areas with similar contamination levels.

1. Introduction

Potentially toxic elements (PTEs) are hazardous to plants and animals and may cause health issues to humans (Ali et al., 2020; Hou et al., 2020). They may be of geogenic and anthropogenic origins, but when they are present in elevated quantities, their source tend to be anthropogenic (Liu et al., 2020; Palansooriya et al., 2020; Pavlovic et al., 2021). Mining is historically a disruptive human activity, in which vast quantities of PTEs are released into neighboring environments. Released PTEs are eventually deposited in the soil (Luo et al., 2020; Gabersek and Gosar, 2021). Over a short period of a few decades, mining activities have been the primary cause of elevated PTEs in the soil of multiple countries, especially in those under rapid industrialization (e.g., China, Xi et al., 2020; Nigeria, Adewumi et al., 2020; Spain, Gallero et al., 2019; Equador, Mora et al., 2019). Presently, historical mining sites are reported to still cause contamination (Mariet et al., 2016). Mining areas with highly elevated PTE contents in soil do not only generate problems for plants, but also enhance the risk to human health through direct soil ingestion. Additionally, crops in close proximity to mining activities are susceptible to the risk of transferring PTEs to humans through the plant (food)-to-human pathway (Antoniadis et al., 2019a). The silver/lead mines of Lavrio, South Attica, Greece is one of the legacy mining sites in southern Europe (Kalyvas et al., 2018).

Presently, Lavrio is experiencing contamination of its soil through the presence of high PTE levels, owing to the past mining activities (Panagopoulos et al., 2009). Underlying rocks contain elevated concentrations of a range of PTE-bearing minerals, mostly containing vast quantities of As, Cd, Sb, Zn, and Ag. Additionally, the ground water is reported to be contaminated with PTEs (Stamatis et al., 2001), as evidenced by contaminated river sediments (Alexakis, 2011). For surface soil, there have been attempts to study various PTEs, mainly targeting Pb as a metal most associated with environmental concern (Korre et al., 2002; Aberg et al., 2001). Excluding the aforementioned studies, most of the literature related to Lavrio has reported on As, Cd, Cr, Cu, Ni, and Zn (Kalyvas et al., 2018). These studies have described the magnitude of the impacts associated with PTEs. However, the studies target areas in close proximity to the mines and do not include urban areas within the town itself, where health risk assessment would be beneficial.

To the best of our knowledge, there are no published scientific studies that report on the presence of PTEs in soils within the town. Similarly, there has not been any study concerning native plant species growing as weeds; these well-adapted species could be good candidates for phytoremediation. Thus, in this study weed species growing in open spaces inside the urban area of Lavrio were collected to assess their PTE levels and the possibility of using them as phytoremediation species, two of which, *Anchusa undulata* and *Avena sterillis*, have never been studied before. Furthermore, because residents of Lavrio cultivate olive trees in their backyards and small vacant plots for consumption, it is essential that the risk to residents be assessed. Additionally, published studies do not describe monitoring PTEs other than As, Cd, Cu, Zn, as well as those constituting the structure of main primary minerals, i.e., Al, Fe, and Mn. Other important elements are overlooked, although they may be of significance in contaminated areas. These elements would include Ag, Co, Hg, Mo, Sb, Se, Sn, Ti, and V.

Hence, this study aimed at thoroughly monitoring the urban area of Lavrio that has not been studied prior to this research. The levels of 19 PTEs (namely, Ag, Al, As, Cd, Co, Cu, Cr, Hg, Fe, Mn, Mo, Ni, Pb, Sb, Se, Sn, Tl, V, and Zn), as well as four plant species growing as weeds, and olive trees inside the town (leaves, olive flesh, and olive cores) were studied. We aimed at achieving this by assessing: (a) the level of the PTE enrichment using contamination indices, (b) the association of elevated toxic elements (As, Pb, Fe, and Zn) with soil colloidal phases using the synchrotron-based X-ray absorption near edge structure (XANES) technique, (c) weeds as potential phytoremediation species, and (d) the PTE-related human health risk based on the soil-to-human and olive consumption-to-human pathways. We measured the concentrations of 19 toxic elements in soils and their uptake by plants, and described their environmental fate and the associated risk to human health.

2. Materials and methods

2.1. Area description and sampling

Lavrio (also often referred to as Lavrion, Laurion or Laurium) is situated at the southernmost tip of the Attica Peninsula, South Greece, approximately 60 km SE of the country's capital city, Athens. The town has a Mediterranean climate of hot-dry summers and wet-mild cold winters, with an average annual temperature of 17.3 °C and an average annual rainfall of approximately 360 mm (Kalyvas et al., 2018). Lavrio is among the oldest mining areas worldwide, with mining activities having been recorded since the second millennium BC. During the classical period of ancient Greece, the town was exploited for its silver due to the presence of rich Ag-bearing ores. Mining activity in the area was revitalized approximately 170 years ago, with metallurgical companies targeting existing mine tailings, which were sufficiently rich in Pb and Ag. Mining and smelting metallurgical activities continued with numerous interruptions until the end of World War II and eventually ceased in the 1970's. In this study, sampling was conducted in the urban area of Lavrio in May 2019, during the period when weeds were abundant. The 35 sample locations used in this study included vacant land, parks and school yards. We collected 35 surface (0–20 cm) soil samples; the map of the area is shown in Fig. 1. At each location, a composite sample of 3–4 subsamples scattered in a space of 10 m^2 were collected using an auger and placed in a clean plastic bag. Between 1 and 3 plant samples were collected at each location by cutting them approximately 10 cm above ground level. The aerial biomass per plant species was collected and placed in separate paper bags. The plant species sampled were *Oryzopsis miliacea* (L.) Asch. and Schweinf, *Anchusa undulata* L., *Malva sylvestris* L., and *Avena sterilis* L. at 35, 16, 9, and 14 locations, respectively. These species were collected as samples owing to their abundance in the area. The soil and plant samples were then transported for analysis to the Laboratory of Soil Science, at the University of Thessaly, in Volos, Greece. In November of 2019, during olive harvesting, we collected olive fruits and leaves from 20 locations in the town. Trees within the town were targeted, typically from house backyards or small—of a few dozens m^2 each—open spaces among houses functioning as "unofficial urban fields." Olive trees at these locations tend to be hand-picked by owners for either table olive preparation and consumption or olive oil extraction. At each location, we sampled 2–3 different neighboring trees and leaves, and their fruits were placed into one composite sample in paper bags and transported to the laboratory for analysis. A total of 55 samples (35 of soil and weeds plus 20 of olive trees) was considered to be an adequate representation of the relatively small urban area of the town of Lavrio.

The soil samples were air dried, ground using a pestle and mortar, and then passed through a 2-mm sieve. The soil samples were subsequently placed in clean plastic vials ready for analysis. The plant samples were washed with tap water, followed by 0.5 M HNO_3, and then rinsed with distilled H_2O. The weeds were dried at 70 °C, until no further weight loss was recorded. Similarly, the olive tree samples were separated into leaves, fruit and cores and dried similarly to the weeds. All plant samples (weeds and the three olive tree parts) were ground to a

fine powder with a non-metallic mill and placed in clean plastic vials. Along with 1 kg of the sieved soil samples, they were then sent to the Department of Soil and Groundwater Management, Wuppertal University, Germany, for the PTE analyses.

2.2. Analytical procedures

The remaining soil samples at the Volos laboratory were analyzed for selected physico-chemical properties according to the standard methods reported by Rowell (1994). These included pH (1:2.5 H_2O), electrical conductivity (1:1 H_2O), equivalent $CaCO_3$ (Bernard calcimeter), organic C (i.e., Walkley and Black methods of wet oxidation with surplus $K_2Cr_2O_7$, back-titrated with $FeSO_4.7\ H_2O$), and particle size analysis (Bouyoucos hydrometer).

All the PTE analyses on the soil and plant samples were performed in the Wuppertal University laboratory. For the pseudo-total concentrations of soil PTEs, a 0.6-g subsample was digested in triplicates in an ETHOS EASY (Milestone, Germany) microwave system, according to the US EPA 3051a (2007). Furthermore, we extracted soils using 1 M NH_4HCO_3 - diethylenetriaminepentaacetic acid (AB-DTPA) (Soltanpour and Schwab, 1977). A sample of 1 g of the plant material was extracted with 20% HCl after being dry-ashed for 5 h at 500 °C in triplicate (Jones et al., 1991). The soil and plant extracts were analyzed for Ag, Al, As, Cd, Co, Cr, Cu, Fe, Mn, Mo, Ni, Pb, Sb, Se, Sn, Tl, V, and Zn in an inductively-coupled plasma optical emission spectrometry (ICP-OES; Ultima 2, Horiba Jobin Yvon, Unterhaching, Germany). The total Hg concentrations in soil and plant samples were directly measured using a Milestone DMA-80 Hg analyzer which has a detection limit of 0.01 ng L^{-1}.

2.3. Quality control and statistical analyses

All the reagents used for extraction and analyses in this study were of analytical grade (high purity reagents), and the standard solutions were purchased from the Merck group (Labmix24 GmbH, Germany). Additionally, all plastic- and glassware was soaked in 3% nitric acid for 24 h and rinsed with deionized water before use. Moreover, all the equipment was regularly and routinely calibrated and data uncertainties were calculated to ensure the accuracy of the extracted and measured data. Quality control of the extraction and analysis efficiency of the pseudo-total content of the studied PTEs in soils was performed using the certified soil reference materials CRM051 and CRM042 obtained from the Sigma-Aldrich Chemie GmbH (Taufkirchen, Germany), and BRM9b, BRM10a, BRM12, and BRM 13 from the Federal Institute for Materials Research and Testing (Berlin, Germany). The average recovery percentage of the studied elements ranged from 89% to 101%. Quality control of the extraction and analysis efficiency of the PTEs content in the plant samples was performed using the certified plant reference materials IPE677 and IPE682 obtained from the International Plant Analytical Exchange evaluating programs for analytical laboratories (Wageningen, Netherlands). We also used the certified plant reference materials BCR-679 and BCR-414 obtained from Labmix24 GmbH, Germany, and produced by the European Commission Joint Research Center, Institute of Reference Materials and Measurements. The average recovery percentage of the studied elements ranged from 89% to 109%. Details on the reference materials are shown in Table SM-1 in the

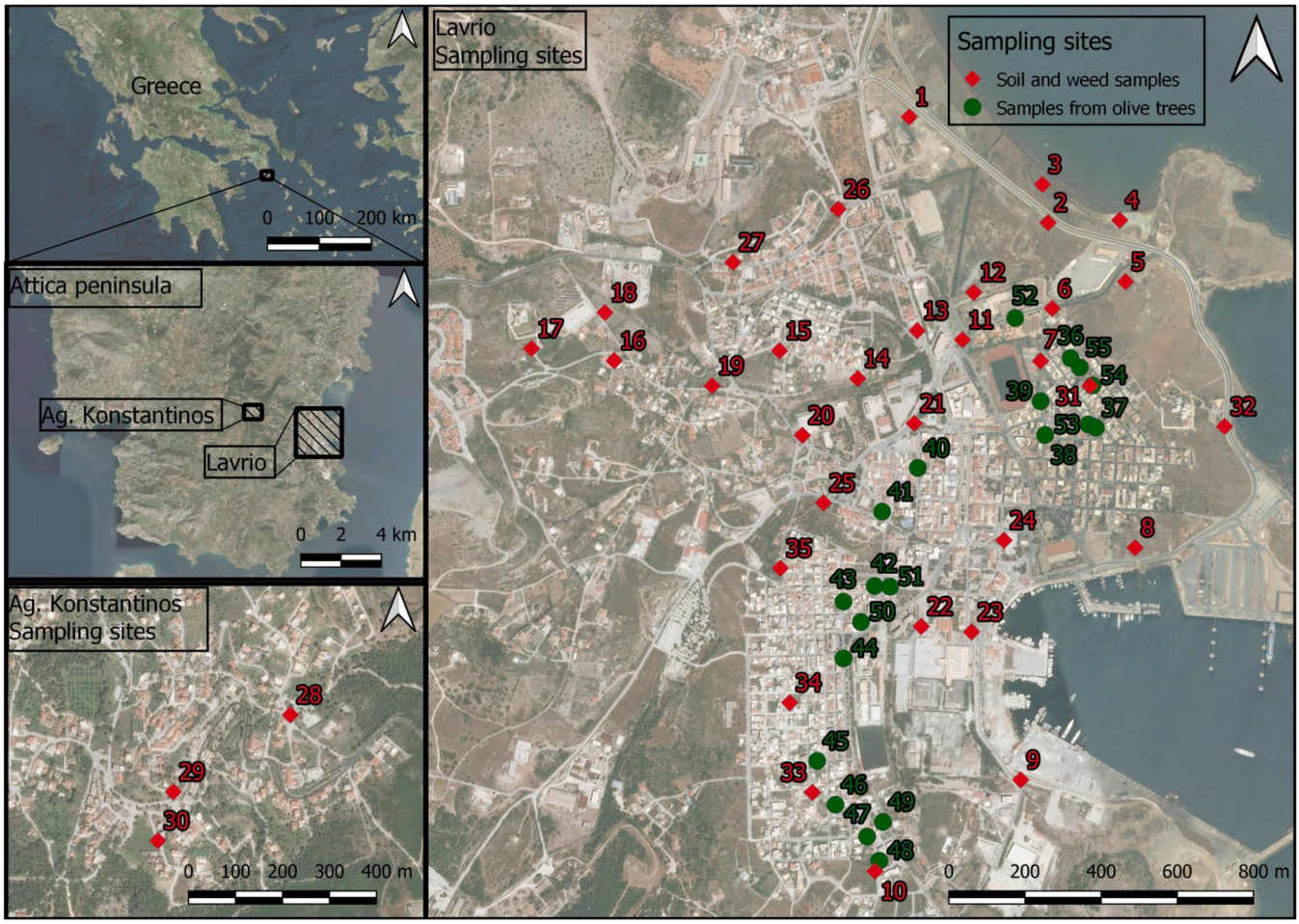

Fig. 1. Map of the urban area of Lavrio with the 35 sampling points of soil and weeds and 20 sampling points of olive trees.

Supplementary material. The validity of the measured data using ICP-OES was ensured by employing measurements of different concentrations (6.25, 12.5, 25.0, 50.0, 100.0, 500.0, and 1000.0 μg L^{-1}) of the PTEs standard solutions (MERCK) in triplicate. The limits of detection (LOD) and quantification (LOQ) of each element were tested and established. Values lower than the LOQ were excluded. The analyses were done in triplicate, followed by the automatic calculation of the average and relative standard deviation (RSD) values using ICP-OES. The maximum RSD between quintuplicates was set to 10.0% and 15.0% for soil and plant samples, respectively, and values above the maximum RSD were excluded from the statistical analyses. The statistical analyses and graphing were conducted using the IBM SPSS Statistics 26 software. Additionaly, we performed one-way ANOVA and Duncan's multiple range test at the level of significance of 95% ($p < 0.05$).

2.4. X-ray absorption near edge structure (XANES) analysis

In four selected soil samples, a XANES analysis was conducted at Beamline 07 A for As, and Beamline 17 C for As, Fe, Zn and Pb, at the National Synchrotron Radiation Research Center, in Hsinchu, Taiwan. The monochromators of the beamlines were calibrated to the absorption *K edge* of As (11867 eV), Zn (9569 eV) or Fe (7112 eV), and the absorption L_3 edge of Pb (13035 eV) for the analysis of the corresponding element. Additional information on the methodology employed (i.e., steps of energy and time for each step) are described in the Supplementary material. A minimum of two scans were collected for individual samples in fluorescent mode using a Lytle detector and then processed for energy calibration, baseline correction and normalization, using the Athena software (version 0.9.23) (Athena, 2005; Ravel and Newville, 2005a). The sources of the materials mentioned below are shown in the Supplementary material (Table SM-2). Linear combination fitting (LCF) was conducted to determine the chemical speciation of As, Fe, Zn, and Pb in the samples using the Athena software with a set of reference spectra (arsenic reference compounds: Goethite-bound As(V), goethite-bound As(III), beudantite, ferrihydrite-bound As(III), ferrihydrite bound As(V), scorodite, and FeAsS; iron reference compounds: Scorodite, ferrihydrite, $FeSO_4$, goethite-like minerals, and siderite; lead reference compounds: $PbCl_2$, humic acid-bound Pb, PbO, $PbCO_3$, and PbS; zinc reference compounds: $Zn(NO_3)_2$, $Zn_3(PO_4)_2$, $Zn(OAc)_2$, Zn $(OH)_2$, ZnS, humic acid-bound Zn, and illite-bound Zn). The LCF procedure was performed using all possible binary combinations of the reference spectra, while not permitting energy shifts in the reference spectra during the LCF. The goodness of fit test was evaluated using the statistical *R* factor, defined as $\sum(\text{data - fit})^2/\sum(\text{data})^2$ (Ravel and Newville, 2005b; see also the "Athena Users' Manual" for details; Athena, 2005). To avoid overfitting, adding a third or fourth reference spectrum to LCF was only allowed when the added spectrum accounted for over 5% of the fitted sample spectrum, and the *R* value of the fitting decreased.

2.5. Use of contamination indices

In this study we calculated various indices based on Antoniadis et al. (2017a), for better comparison with other studies. First, to calculate the soil-to-plant transfer with the unitless transfer coefficient (TC) we followed:

$$TC = C_P/C_S \quad (1)$$

where C_P = PTE concentration in the plant; C_S = pseudo-total PTE in the soil.

To calculate the Contamination Factor (*CF*):

$$CF = C_S/C_{RefS} \quad (2)$$

where C_{RefS} = PTE background concentrations ("*world soil average*," Kabata-Pendias, 2011, p. 41).

To calculate the Pollution load index (PLI):

$$PLI = (CF_1 \times CF_2 \times \ldots \times CF_n)^{1/n} \quad (3)$$

where 1, 2, …, *n* are the studied PTEs.

To calculate the Enrichment Factor (*EF*):

$$EF = (C_S/Al_S)/(C_{RefS}/Al_{RefS}) \quad (4)$$

where Al_S is the Al concentration in contaminated soils and Al_{RefS} is the background Al. *EF* is categorized into enrichment classes: I: $EF < 1.5$ (pristine soil), II: $EF = 1.5$–3 (soil with "minor"), III: $EF = 3$–5 ("moderate"), IV: $EF = 5$–10 ("severe"), V: $EF > 10$–20 ("extreme" or "very severe").

2.6. Health risk assessment

2.6.1. Non-carcinogenic risk indices

Concerning the "soil-to-human" pathway, we calculated ingestion, D_S (mg kg^{-1} BW d^{-1}):

$$D_S = C_S \cdot \frac{IngR \cdot EF \cdot ED}{BW \cdot AT} \cdot 10^{-6} \quad (5)$$

where IngR = Ingestion rate (100 mg d^{-1}); EF = Exposure frequency (350 d yr^{-1}); ED = Exposure duration (30 yr); BW = Body weight (70 kg); and AT = Averaging time (EDx365 d=10,950 d).

Then, Hazard Quotient (HQ):

$$HQ_S = D_S/RfD \quad (6)$$

where RfD (mg kg^{-1} BW d^{-1}) is reference dose (values shown in Table SM-3; Appendix A).

Subsequently, Hazard Index:

$$HI_S = \Sigma(HQ_S) \quad (7)$$

Concerning the "food-to-human" pathway: D_F (units same as for D_S):

$$D_F = C_F \cdot \frac{MIDVC \cdot EF \cdot ED}{BW \cdot AT} \cdot 10^{-6} \quad (8)$$

where C_F is PTE concentrations in table olive fruits in mg kg^{-1} fresh food, and MIDVC is the mean individual daily food consumption, obtained as 11.23 g of table olives per capita per day (FAO, 2020).

Similar to the soil pathway, we assessed the induced from food Hazard Quotient (HQ_F):

$$HQ_F = D_F/TDI \quad (9)$$

where TDI is the maximum tolerable daily intake (same units as D_F, values shown in Table SM-3; Appendix A).

Then, the associated Hazard Index (HI_F):

$$HI_F = \Sigma(HQ_F) \quad (10)$$

2.6.2. Indices related to carcinogenic risks

The unitless soil-associated Cancer Risk (CR) was assessed as follows:

$$CR_S = D_S \text{ x } OSF \quad (11)$$

where OSF is the oral slope factor.

Here D_S substitutes ED with LT=Lifetime (70 yr).

Then, food-associated risk:

$$CR_{Fi} = D_F \text{ x } OSF \quad (12)$$

OSF values are shown in Table SM-3 (Appendix A).

In all equations the values were extracted from USEPA (2002, 2016, 2017).

3. Results and discussion

3.1. Soil characterization

The soil samples were predominantly alkaline (average pH = 7.78), and calcareous (average $CaCO_3$ = 7.28%), with low organic C (average 1.83%), which is typical of Mediterranean climates. Soils had relatively low clay content (average of 15.3%, sand 64.3% and silt 20.4%), but were rich in total "free" oxides (average Fe oxides = 7040.01,Al = 868.84, and Mn = 1391.80 mg kg^{-1}, with average total oxides 183.59 mmol kg^{-1}). The total mean for Fe was 41,987 mg kg^{-1}, Al was 13,800 mg kg^{-1}, and Mn was also relatively high, at 2194 mg kg^{-1} (Table 1, and Table SM-4, Appendix A).

3.2. Pseudo-total content of trace elements in soil

We found that the majority of the measured PTEs (Table 2) was elevated above their background levels (reported as "*world soil average*," Kabata-Pendias, 2011, p. 41). The average value (mg kg^{-1}) for Ag was 8.78 vs. background of 0.13, indicating a serious enrichment, not unexpected for a Ag-mining area. Arsenic had an average concentration of 1522.34 vs. background of 6.83 mg kg^{-1}, similar to Cd, which was elevated by two orders of magnitude compared to the background (39.59 vs. 0.41 mg kg^{-1}). Other elements with elevated average values included Pb (average 7844 vs. background of 27 mg kg^{-1}), Sb (76.68 vs. background of 0.67 mg kg^{-1}, a two-order-of-the-magnitude enrichment), and Zn (6458 vs. background of 70 mg kg^{-1}). Among the rest of the studied elements, some were elevated above their background levels, but not as dramatically (Co, Cr, Cu, Ni, Sn, and Tl). Among the studied PTEs, average values were below their background in the case of Mo (detected in 13 out of the 35 samples), Se (detected in only 4 samples), and V (average 51.77 vs. background of 129 mg kg^{-1}), while Hg was barely detected in any of the samples analyzed. PTEs with average values exceeding all the reported limit values were As, Cd, Pb and Zn, whereas Cu and Ni exceeded their European Union (EU) limits of 140 and 75 mg kg^{-1}, respectively (CEC, 1986). These results confirm the extent to which the soils are enriched with PTEs.

The EF corroborated these findings. Among the studied elements, seven indicated "extreme enrichment" with an EF > 20, while others scored higher values. For Pb, the average EF was 431, As = 423, Sb = 180, Cd = 156, Zn = 145, Ag = 102, and Tl = 20.3 (Fig. 2). Four elements showed "severe enrichment": Mn = 7.73, Cu = 7.17, Sn = 6.04, and Ni = 5.94. The remaining elements fell within the categories of less severe enrichment: Cr (2.87) and Co (1.82) were of "minor enrichment," while Se (0.54), V (0.50) and Mo (0.40) were found at levels typical to "pristine soil." These findings were similar to another contamination index, the CF (Fig. SM-1, Appendix A).

There is an absence of literature that describes multiple elements at these enriched levels in soil (Table 2). This is indicative of how mining activities unearthed and deposited excess PTEs such as Ag, As, Cd, Pb, Sb, Tl, and Zn in surface layers. There have been similar studies in the literature that have reported high levels of such PTEs. Particularly Yildirim and Sasmaz (2017) studied an area with reportedly the richest Ag deposits in Turkey. They found that the mean Ag in the soil was 37.78 (max. was 127), mean As was 4771 (max. 14,662), and mean Pb was 4320 (max. 13,556; all values in mg kg^{-1}). Similarly, Zhou et al. (2020) studied a farmland adjacent to a legacy Zn smelting area in China, and reported Ag levels similar to our results of 6.95 mg kg^{-1}, while As, Cd, Pb and Zn levels were highly elevated, but not close to the values we reported; Tl was close to its background levels. Furthermore, Oyarzun et al. (2011) studied a Pb-Ag-Zn mine area in Spain and reported that in 12 soil samples the maximum value of Ag was 36.0 mg kg^{-1} (max. 38.70 in our study), Pb = 6010 (max. 31,332 in our study), Zn = 5250 (vs. 58, 726 here), and Sb = 174 (vs. 298 here; all values in mg kg^{-1}). However, there are earlier reports on Ag mining areas in which Ag was discovered to have very low values, for example, studies by Aide (2009) on soils close to Pb-Zn-Cd-Ag-In mines in Missouri, United States of America, and Huang et al. (2020) on soils close to a Pb-Zn-Ag mine. Some studies did not consider Ag in their analysis related to Ag mining activities, as was the case with Jung (2001) and Lee et al. (2001), both reporting results for soils close to a Au-Ag mine in Korea.

The enrichment of these PTEs was likely geogenic, because Lavrio is still abundant in minerals that initially attracted the mining activities. Such minerals are the sulfuric Ag-bearing galena (PbS), sphalerite (ZnS), and arsenopyrite (FeAsS) (Pappa et al., 2018). There are also prototype minerals identified as "type locality," first found in-situ, including georgiadesite—$Pb_8(AsO_4)_2OCl_7(OH)$, thorikosite—$Pb_3(Sb^{III}As^{III})O_3(OH)Cl_2$, and fiedlerite—$Pb_3Cl_4F(OH)\cdot H_2O$.

For Tl, there are few reported cases in the literature that describe significant Tl contamination. For example, Huang et al. (2018a) reported high Tl content of up to 8 mg kg^{-1} (the average was 6.07 in our study, with a 90th percentile at 12.19 mg kg^{-1}). There are other studies that reported extremely high Tl concentrations attributed to either natural (Xiao et al., 2004a) or anthropogenic origins (Xiao et al., 2004b; Funes Pinter et al., 2018). For Sb, with few reported cases in the literature, our study determined that theses Sb levels are attributed to the naturally occurring Sb-bearing minerals in the area. Highly elevated Sb concentration are typically reported in soils in the vicinity of Sb mines, as in the case of Tang et al. (2020). They reported an average soil Sb level of 4368 mg kg^{-1} in an Sb mine in Xikuangshan, China (our study showed average soil Sb levels of 76.68 mg kg^{-1}, two orders of magnitude), while the levels of As and Pb were much lower than those in our study. Similarly, Mbadugha et al. (2020) reported maximum Sb levels in an historical mining site in Scotland of 1504 mg kg^{-1} (in our study, the maximum Sb was 297.86 mg kg^{-1}), while co-related As had a maximum value of 15,490 mg kg^{-1} (max. As = 10,886 here). Moreover, in a review concerning Sb contamination in Poland, maximum levels were reported in an Sb mine with concentrations of 5600 mg kg^{-1} (Lewinska and Karczewska, 2019). Contrary to these reports, other studies on highly polluted soils reported Sb levels of much lower concentrations. These are described in Zhang et al. (2019) (with Sb = 18.10), (with Sb=14.8 in a Tl-mining site with Tl = 44.8), and Teng et al. (2020) (with Sb = 67; all

Table 1
Descriptive statistics of selected physico-chemical properties of the soils studied in the urban area of Lavrio, southern Greece.

	Sand	Clay	OC	$CaCO_3$	pH	EC	Al-ox	Fe-ox	Mn-ox	Oxides	Fe-t	Al-t	Mn-t	S-t
	%				—	μS cm^{-1}	mg kg^{-1}			mmol kg^{-1}	mg kg^{-1}			
Min	40	4	0.51	2.44	7.25	147	129.64	396.9	98.3	13.7	2575.0	2078.0	81.3	344.6
10th-perc	49	7	0.81	7.35	7.44	186	361.70	1218.0	282.2	50.5	17,439.0	7623.0	465.6	543.2
50th-perc	64	14	1.83	13.13	7.77	365	837.72	3413.8	1109.8	119.7	33,187.0	13,117.0	1475.1	1228.2
Average	64	15	2.04	14.56	7.78	784	868.84	7040.0	1391.8	183.5	41,987.0	13,800.0	2194.3	5767.9
90th-perc	80	24	3.90	27.85	8.12	1599	1331.15	12,570.6	3156.9	297.7	77,485.0	20,312.0	2585.9	9509.8
Max	91	34	4.80	35.78	8.40	6954	2071.88	51,680.0	5656.9	1036.9	171,339.0	31,358.0	13,981.1	92,193.4
Skewness	0.07	0.83	0.99	1.03	0.04	3.78	0.60	3.41	1.90	3.14	2.47	0.81	3.00	5.8

Al-t. Fe-t, Mn-t, S-t = total contents of Al, Fe, Mn, and S.
Al-ox. Fe-ox, Mn-ox = Total "free" oxides in mg kg^{-1}.
Oxides = The sum of Al, Fe, and Mn oxides in mmol kg^{-1}.

Table 2
Pseudo-total concentrations of potentially toxic elements (mg kg^{-1}) in the urban area of Lavrio, southern Greece.

	Ag	As	Cd	Co	Cr	Cu	Mo	Ni	Pb	Sb	Se	Sn	Tl	V	Zn
Min	0.09	7.30	0.17	1.04	7.33	8.29	0.00	7.21	36.17	0.75	0.00	0.99	0.00	8.09	56.19
10th-perc	0.64	120.35	2.79	6.89	32.17	26.43	0.00	37.64	820.19	11.24	0.00	3.06	1.84	22.66	581.97
50th-perc	5.36	837.05	22.57	14.44	116.58	104.00	0.00	114.29	4624	43.26	0.00	6.95	4.24	39.55	3561
Average	8.78	1522.3	39.59	13.85	120.27	166.01	0.32	119.49	7844.0	76.68	0.05	9.82	6.07	41.77	6458
90th-perc	21.39	3548.57	79.78	21.13	191.94	307.48	1.00	213.97	24,221	188.91	0.08	18.44	12.19	65.31	11,501
Max	38.70	10,885.86	287.70	25.29	310.82	1273.32	2.02	280.03	31,332	297.86	0.62	42.93	30.69	102.95	58,726
Skewness	1.69	2.83	3.30	-0,11	0.73	3.87	1.94	0.68	1.52	1.49	3.03	2.18	2.68	0.96	3.98
BG	0.13	6.83	0.41	11.3	59.5	38.9	1.1	29	27	0.67	0.44	2.5	0.5	129	70
EU	–	–	3	–	–	140	–	75	300	–	–	–	–	–	300
TAV	40	65	20	100	450	500	20	150	300	–	10	50	–	340	1500
MAC	–	20	5	50	200	150	10	60	300	–	–	–	–	150	300

BG=Background as reported by Kabata-Pendias p. 41) (2011).
EU=Limits according to the European Union Directive (CEC, 1986).
TAV=Maximum value of the range of Trigger Action Values as reported by Kabata-Pendias p. 24) (2011).
MAC=Maximum value of the range of Maximum Allowable Concentrations as reported by Kabata-Pendias p. 24) (2011).

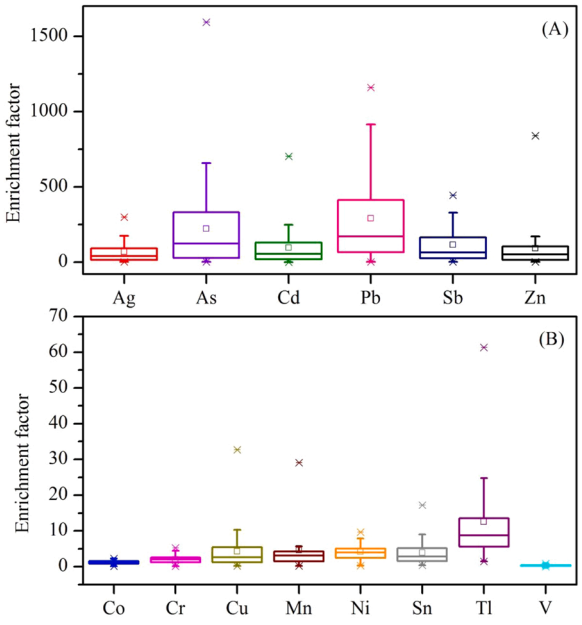

Fig. 2. Enrichment factor of 35 soil samples in the urban area of Lavrio, southern Greece.

values in mg kg^{-1}). Antimony is highly related to As, as confirmed by the significant correlation between the two elements ($r = 0.519$, $p < 0.01$; Table SM-5, Appendix A): both are metalloids with similar chemical behavior and lithogenic occurrence. Both elements are redox-sensitive (they have dual species with +III and +V oxidation numbers) and found as anion species in soil solution, with Sb predominantly present as $Sb^{V}(OH)_6^-$ and As as $As^{III}O_3^{3-}$ and $As^{V}O_4^{3-}$ (Teng et al., 2020). Elements such as Se, Sb, Mo, Sn and Ag are scarcely measured in similar monitoring studies (Mykolenko et al., 2018, reporting Sb). Often in cases of soil contamination, the study of these elements is ignored (Rodriguez-Iruretagoiena et al., 2016). The total elemental content was found to be influenced by some soil properties, including the oxides content (correlated with As, Fe, Mn, and Tl), clay content (Al), organic C (Cd and Sb), and $CaCO_3$ (Ag, Al, Fe, Mo, Pb, Sb, Se, and Zn; data not shown).

Our study found contamination by multiple elements that was confirmed by the PLI of 11.32 (data not shown), much higher than that in many other areas reported elsewhere (Gabersek and Gosar, 2018). In other studies reporting significant contamination cases, the PLI has rarely recorded high values as those in our study. For example, Shaheen et al. (2020) reported a PLI ranging from 1.1 to 5.2 in contaminated soils in Egypt and Germany; Hadjipanagiotou et al. (2020) reported a PLI of 2.4 in a Cu mine in Cyprus, while Sofianska and Michailidis (2016) reported a mean PLI = 3.1 in a Mn mine, and Rinklebe et al. (2019) reported an average PLI of 1.73 in highly contaminated soils in Germany. Studies on contaminated soils have even reported of PLI of less than 1.0 (Shahmoradi et al., 2020).

To investigate the geochemical characteristics of important elements we studied the XANES spectra of Fe, As, Pb, and Zn in four samples with highly elevated contents (#12, #18, #25, and #29; Fig. 3, Table 3). For Fe, it was found that the most predominant species was goethite-like minerals (goethite idealized formula, $Fe^{III}O(OH)$), a known abundant mineral of the study area, and also a predominant oxide in the clay fraction of the soil. This phase accounted for 68% of bound Fe in sample #12, 64% in #18, 69% in #25% and 72% in #29. The second dominant form of Fe was $FeSO_4$ (the association ranged from 14% for sample #29 36% for #18), a soluble mineral crystallized in the presence of abundant S^{VI}, which is readily found in the area due to the presence of S-bearing ores. The third mineral associated with Fe was scorodite (in samples #12, 25, and 29). The occurrence of other Fe phases was tested using the best fits of the samples but no improvement was obtained. Considering the sensitivity and resolution of XANES, those Fe forms were not included in the LCF to avoid over-fitting, even though their occurrences could not be completely ruled out. As for the predominant forms of Fe (i.e., goethite-like minerals, $FeSO_4$ and scorodite), the occurrence of these secondary minerals may have resulted from the on-site transformation of pyrite, which is a common mineral in mining ores.

The LCF analysis revealed that As was associated predominantly with scorodite ($Fe^{III}As^{V}O_4.2\,H_2O$), an important primary As-bearing mineral of the area. This mineral accounted for 60% of the As in sample #12, 77% in #18%, and 78% in #25 and #29. Scorodite was followed by As (V)-bearing goethite (40% of total binding in sample #12, 23% in #18, 21% in #25% and 7% in #29). Arsenopyrite, i.e., FeAsS, an abundant mineral in the study area, was also found in sample #29. Previous studies indicate that the oxidation of FeAsS could lead to the formation of scorodite, accompanied by As-bearing Fe oxide and sulfate (such as beundantite) (Majzlan et al., 2014; Yang et al., 2020). The association of As with these minerals revealed that As-associated sulfide minerals could be the origin of As in the soils. Meanwhile, scorodite is metal-stable and thus could lead to the formation of Fe oxides (Bluteau and Demorpoulos, 2007; Langmuir et al., 2006; Yang et al., 2020). The LCF results also indicated that the predominant association of As with Fe in soils is through precipitation and sorption, represented by scorodite and As-bearing goethite, respectively. Although the association of As with other metals cannot be completely ruled out, the inclusion of any other reference materials did not further improve the LCF results, indicating their relatively insignificant contribution to As occurrence in the soil. Owing to the limitations of the sensitivity and resolution of XANES, As-bearing goethite may represent As sorption with various hydrous Fe oxides and similar coordination environments. Compared with the

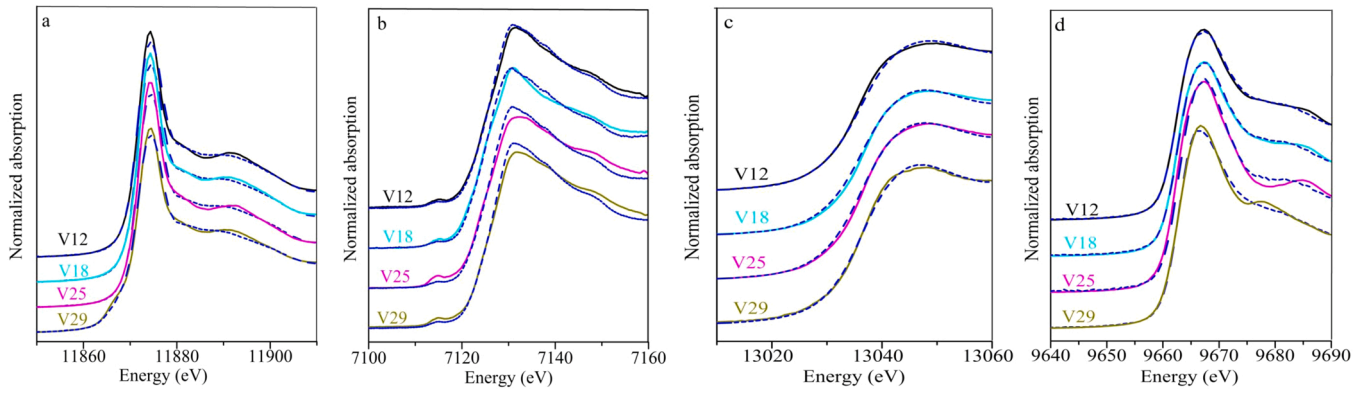

Fig. 3. The arsenic K-edge (a), iron K-edge (b), lead L_3-edge (c), and zinc K-edge (d) X-ray absorption near edge structure (XANES) spectra of the selected soil samples (solid lines, V12, V18, V25, V29) and their linear combination fitting spectra (blue dash line).

Table 3
The linear combination fitting results of the X-ray absorption near edge structure (XANES) of As, Fe, Pb, and Zn of the 4 selected soil samples, V12, V18, V25 and V29.

As speciation		Scorodite	Goethite_As (V)	FeAsS	*R*-factor
	V12	60%	40%	–	0.003
	V18	77%	23%	–	0.004
	V25	78%	21%	–	0.002
	V29	78%	7%	17%	0.004
Fe speciation		$FeSO_4$	goethite	Scorodite	*R*-factor
	V12	22%	68%	10%	0.003
	V18	36%	64%	–	0.004
	V25	24%	69%	6%	0.007
	V29	14%	72%	13%	0.006
Pb speciation		Pb_humic acid	PbO	$PbCO_3$	*R*-factor
	V12	85%	13%	–	0.001
	V18	67%	11%	17%	0.002
	V25	82%	8%	13%	0.001
	V29	76%	0%	27%	0.001
Zn speciation		Zn_illite	$Zn(OH)_2$	Zn_humic acid	*R*-factor
	V12	27%	36%	34%	0.0005
	V18	36%	30%	31%	0.0005
	V25	60%	8%	29%	0.005
	V29	9%	6%	84%	0.002

precipitate phases, sorbed As has lower stability and thus may contribute to soil As availability.

Lead was found to be associated predominantly with humic substances. This association explained 67% (sample #18) to 85% (sample #12) of bound Pb; this is not unexpected for Pb, an element known for its strong retention with organic matter due to its tendency of forming strong organo-metallic complexes, also a possible source of available Pb. Apart from humic substances, PbO and $PbCO_3$, two sparingly soluble solid phases in alkaline soils, such as in our study area, were also found to have an important role in binding Pb (PbO in samples #12, 18, and 25; $PbCO_3$ in #18, 25, and 29). Lead (II) oxide is the stable and insoluble end product of the weathering of galena (PbS) accelerated under oxidation conditions (i.e., in aerated surface soils such as our study area) (Wang et al., 2021). This explains the limited bioavailability of Pb, as noted in our study for plant uptake. Additionally, the presence of humic substances hinders Pb transformation to its secondary species (Liu et al., 2018).

As for the fourth XANES-explored metal, Zn, we found that three solid phases had nearly evenly distributed predominance in its binding in samples #12 and #18: (a) illite (a 2:1 clay phyllosilicate with relatively high charge of ca. 0.9 mol_c ½mol^{-1}, but a rather low ion exchange capacity of 40 $cmol_c$ kg^{-1}), (b) its insoluble hydroxide species $Zn(OH)_2$, known to be abiding in alkaline environments, and (c) humic substances. In sample #25, illite was predominant (60%), while humic substances were predominant (84%) in sample #29.

3.3. Trace elements in weeds and olive trees

The trace element availability was reflected in the uptake by localized weeds. We selected two species (*Anchusa undulata* and *Avena sterilis*) not previously studied. Among the other two species, *Oryzopsis miliacea* was found to have been studied only once in the past decades (Schwab et al., 1983), and *Malva sylvestris*, owing to the fact that it may be used for medicinal purposes, was studied in eight similar studies (search retrieved through Scopus). We analyzed all previously cited PTEs in *O. miliacea* (results shown in Table 4), as the most promising among the sampled weeds, while the other three species were measured for Cd, Cu, Fe, Mn, Pb, and Zn only (Table SM-6). It was found that, as also predicted by the DTPA extractions (Table SM-7; Appendix A), Mo and Tl were below the level of analytical detection. For the physiologically essential elements (Fe, Mn, Zn, Cu, and Ni), we found high concentrations. This was not unexpected as it is common for weeds growing in soils with extremely elevated levels of essential metals to absorb rather high concentrations. Among the non-essential elements, Pb was found at very high levels that averaged 19.57 (ranging from zero to 98.92 mg kg^{-1}), while the average As content was high (3.04, with maximum of 10.12 mg kg^{-1}) among the 35 sampling points. Concerning Ag and Sb, two elements of particular interest to that specific locality, it was found in detectable concentrations, although at low average levels of 0.32 and 0.36 mg kg^{-1}, respectively. This finding has not been previously reported in similar studies, and signifies the ability of these elements to be transferred to plants in highly enriched soils, however low this transfer may be. The soil-to-plant transfer coefficient is reported and discussed in the Appendix (Table SM-8).

Furthermore, we investigated the impact of soil contamination on olive trees. Within the town of Lavrio, we collected olive tree leaves, seeds, and fruits (Table 5) during the olive ripening period from 20 sampling locations. In the olive fruit measurements, we detected Hg above the analytical quality level; thus, we report this element. For reasons of better arrangement in Table 5, we excluded Tl, which was found below the level of quality, from the presentation. We found that for the physiologically essential elements, their average values in leaves were not high (Fe = 223, Mn = 43, Cu = 7.3, Zn = 53, and Ni = 3.32 mg kg^{-1}), although some particular areas may indicate toxicity problems (e.g., maximum Fe was 398 mg kg^{-1}, a value likely exhibiting toxicity). For the non-essential elements, the average As and Pb levels were similar to those in *O. miliacea* (As = 4.42, Pb = 22.34 mg kg^{-1}), while Ag, Cd and Sb levels were higher in olive tree leaves. As for the olive seeds, all PTE levels were considerably lower, for both essential

Table 4
Potentially toxic elements in *Oryzopsis miliacea* aboveground biomass (mg kg^{-1}) in the urban area of Lavrio, southern Greece.

Concentration	Ag	Al	As	Cd	Co	Cr	Cu	Fe	Mn	Mo	Ni	Pb	Sb	Se	Sn	Tl	V	Zn
Min	0.00	44.48	0.00	0.00	0.00	0.90	3.10	49.18	11.20	ND	2.72	0.00	0.00	0.00	0.00	ND	0.00	19.05
10th-perc	0.00	67.09	0.00	0.35	0.46	1.39	4.03	73.75	17.99		3.33	4.10	0.00	0.00	0.00		0.00	26.73
50th-perc	0.35	110.23	2.65	0.57	0.60	2.13	5.53	133.35	23.12		4.83	12.97	0.00	1.85	1.00		0.00	43.88
Average	0.32	150.23	3.04	0.69	0.59	2.32	5.95	169.61	26.82		5.26	19.57	0.36	1.48	0.87		0.38	57.22
90th-perc	0.52	278.23	6.47	1.15	0.73	3.46	7.86	265.40	41.21		7.83	35.20	1.36	3.08	1.72		1.63	93.80
Max	0.60	765.83	10.12	1.28	1.10	6.83	13.70	710.00	61.02		8.97	98.92	1.70	3.87	2.03		1.95	191.17
Skewness	-0.89	3.26	0.71	0.28	-0.56	2.30	1.79	2.64	1.44		0.60	2.50	1.14	0.03	-0.18		1.42	1.94

ND: Non detected.

and non-essential elements. This was probably because trace elements are mostly immobile within the aerial tree parts; thus, from the leaves, where they are initially stored after uptake, they are scarcely transferred through the phloem (Zaanouni et al., 2018). The same was found by Gurel and Basar (2014), who investigated nutrient and non-essential trace elements in olive leaves and fruits. Rarely in the literature have olive trees been investigated as an index of soil contamination as done in this study. Olive trees are generally only investigated when organic amendments are applied to soil (Tsadila et al., 2009, although total soil content in PTEs was very low), or in studies reporting the nutrient status of the tree (Petousi et al., 2015; Bargagli, 1995). However, even in these cases, olive seeds were not investigated. Therefore, our study is the first to describe the presence of PTEs in olive seeds.

Olives were also investigated in an attempt to assess the degree of PTE transfer to a major food product (table olives). The analysis in oil was not undertaken owing to evidence from the literature, which reported no significant PTE content was to be expected (Fourati et al., 2017). Additionally, there was a comparison of the measured values with those reported as maximum allowable limits for olive products in various countries and legislations (Table 5). For olives, the values we report are in fresh weight; thus, such comparisons may be feasible (legal limits are based on consumption of food in the normal state, as "on the table," or "ready to eat"). The contents were well above those reported elsewhere (Tuna and Gecgel, 2011). Cadmium levels surpassed the legal limit of 0.05 mg kg^{-1} fresh weight in the EU ("vegetables and fruit," section 3.2.15, Directive 629/2008; CEC, 2008) in all samples, with maximum levels climbing up to 0.55 mg kg^{-1}, which are 11 times higher than the limit. For Pb, the limits in the EU ("fruit, excluding berries and small fruits," section 3.1.12, Directive 1881/2006; CEC, 2006) and Australia/New Zealand ("fruits," FRLI, 2015) are both set at 0.10 mg kg^{-1}. The concentrations found in our study surpassed this limit for half of the sampled areas. The limit set by the Codex Alimentarius Commission ("table olives," FAO/WHO, 2017) is more relaxed, at 0.40, but it was still surpassed in 9 out of the 20 sample locations. The limit in China ("fruit products," concerning "fruits processed with vinegar, oil and salt," GB2761/2012, accessed via USDA, 2014) of 1.00 mg kg^{-1} was surpassed in eight of our samples. Our results signify the considerable risk to human health of the chronic consumption of table olives cultivated in Lavrio. The uptake behavior of olive trees may well be explained by the characteristics of various biochemical processes in the rhizosphere, as follows: the uptake of some of the studied elements may have been influenced by antagonisms caused by similar chemical behavior of some elements that have a net effect in nutrient acquisition by the olive trees. The high As concentration in the soil resulted in an average leaf content value of 4.42 mg kg^{-1}, an extremely high concentration; however, being a typically non-mobile element in plant, phloem mobilization was limited, resulting in an average content in olive fruits of only 0.73 mg kg^{-1} (Table 5). Similarly, the antagonisms between Cd and Zn may have resulted in relatively low Zn concentrations being absorbed compared to the extreme soil Zn contents. This may well be the result of a high Cd concentration being concurrently absorbed (average Cd content in leaves 1.19 mg kg^{-1} vs. 52.55 of Zn).

3.4. Health risk assessment

Health risk assessment (HRA) is a widely used risk analysis tool that interlinks PTE concentrations in soils and plants with human health. It allows for better comparison between studies and is a simple method to assess potential risk. HRA was based on two scenarios of exposure: "soil-to-human" and "food-to-human." Hazard quotients (HQ) higher than unity indicate significant health risk for conditions other than cancer (Fig. 4 presents the most highly scoring PTEs; all studied PTEs are presented in Fig. SM-2). Concerning the soil ingestion pathway, our results indicate that As was by far the most offensive element (average As HQ = 6.95). Among the other extremely enriched elements found in the soil (Cd, Pb, Sb, Tl and Zn), Pb also had a HQ score of well over unity (3.07),

Table 5
Potentially toxic elements in olives parts (leaves, cores and flesh) (mg kg^{-1}; Hg in μg kg^{-1}) in the urban area of Lavrio, southern Greece, and limit values for table olives by Institutions around the globe. Olive leaves and cores are reported in mg per kg dry weight, while olive flesh concentrations are reported in mg per kg fresh weight for reasons of better comparison with the reported limit values (also given in fresh weight). Parentheses in the limit values denote the number of cases surpassing this maximum limit values out of the 20 measured olive trees.

	Ag	Al	As	Cd	Co	Cr	Cu	Fe	Hg	Mn	Mo	Ni	Pb	Sb	Se	Sn	V	Zn
Leaves																		
Min	0.00	59.36	2.20	0.78	0.74	0.96	5.73	95.64	5.70	19.93	0.00	1.90	3.81	0.00	0.00	0.00	0.00	32.29
10th-perc	1.04	93.45	2.32	0.79	0.83	1.05	5.92	123.25	18.56	24.50	0.00	2.18	8.29	0.00	0.00	0.00	0.00	34.07
50th-perc	1.26	157.36	3.56	0.99	1.11	1.54	7.13	201.25	23.44	45.61	0.00	2.39	16.40	0.71	2.45	0.80	0.00	44.56
Average	1.31	179.61	4.42	1.19	1.07	1.67	7.31	222.93	25.41	43.41	0.00	3.32	22.34	1.09	2.02	0.68	0.55	52.55
90th-perc	1.71	286.58	6.70	1.75	1.24	2.30	8.53	336.50	34.44	57.99	0.00	6.22	44.18	2.89	3.54	1.32	1.91	79.65
Max	1.98	325.17	12.22	2.19	1.48	2.95	10.16	398.17	49.30	64.54	0.00	7.11	53.60	3.67	4.05	1.62	2.30	84.78
Skewness	-1.48	0.47	2.11	0.96	0.13	1.01	0.82	0.42	0.63	-0.37	NR	1.52	1.15	0.71	-0.46	-0.03	1.14	0.60
Cores																		
Min	0.62	2.70	0.00	0.43	0.00	0.89	4.13	17.43	0.04	4.08	0.00	1.33	0.00	0.00	0.00	0.00	0.00	13.97
10th-perc	0.76	5.40	0.00	0.43	0.00	1.32	4.66	19.77	0.05	4.66	0.00	1.60	0.00	0.00	0.00	0.00	0.00	17.04
50th-perc	0.93	11.57	0.38	0.66	0.57	2.38	5.48	30.14	0.06	5.85	0.76	2.05	0.00	0.00	0.43	0.00	0.00	31.81
Average	0.90	11.91	0.88	0.63	0.58	3.14	5.72	35.80	0.06	5.86	0.66	2.16	1.00	0.41	0.88	0.42	0.00	33.31
90th-perc	1.11	17.70	2.14	0.76	1.00	3.44	6.78	35.91	0.08	6.88	0.92	2.84	3.65	1.62	2.08	1.18	0.00	55.65
Max	1.13	28.25	2.53	0.90	1.58	16.09	7.98	155.65	0.10	8.22	1.27	3.85	4.72	2.40	2.42	1.28	0.00	63.08
Skewness	-0,01	1.19	0.41	0.03	0.52	3.66	0.56	3.75	0.90	0.37	-0.96	1.57	1.38	1.84	0.31	0.58	NR	0.68
Flesh																		
Min	0.42	2.77	0.00	0.25	0.12	0.00	1.26	5.49	5.49	1.26	0.00	0.46	0.00	0.00	0.00	0.00	0.00	11.10
10th-perc	0.44	4.59	0.46	0.29	0.16	0.24	1.73	8.16	8.16	1.64	0.00	0.49	0.00	0.00	0.00	0.00	0.00	11.34
50th-perc	0.51	7.66	0.70	0.40	0.24	0.42	2.58	15.19	15.19	2.37	0.00	0.80	0.86	0.64	0.60	0.11	0.00	14.98
Average	0.52	9.01	0.73	0.39	0.25	0.44	2.68	17.94	17.94	2.42	0.13	0.83	1.04	0.57	0.44	0.17	0.04	17.11
90th-perc	0.59	15.76	1.16	0.49	0.34	0.80	3.77	30.83	30.83	3.60	0.31	1.05	2.76	1.23	0.94	0.42	0.14	27.60
Max	0.66	18.78	1.40	0.55	0.37	0.96	4.83	42.46	42.46	3.94	0.42	2.04	3.58	1.51	1.11	0.50	0.39	29.46
Skewness	0.46	0.84	0.01	-0.05	-0.01	0.57	0.87	0.98	0.98	0.69	0.48	2.11	0.99	0.39	0.04	0.42	2.62	1.02
EU[a]				0.05 (20)									0.10 (10)			200 (0)		
FAO/WHO[b]													0.40 (9)			250 (0)		
China[c]													1.00 (8)			250 (0)		
Australia/NZ[d]													0.10 (10)			250 (0)		

NR: Not relevant.

[a] For the European Union, Cd concerns "vegetables and fruit" (section 3.2.15, Directive 629/2008). Pb concerns "fruit, excluding berries and small fruits" (section 3.1.12, Directive 1881/2006). Sn concerns "canned foods other than beverages" (section 3.4.1, Directive 1881/2006).

[b] Codex Alimentarius Commission (FAO/WHO, 2017): Pb concerns "table olives" (p. 51 of the cited document). Sn concerns "canned foods other than beverages" (p. 55 of the cited document).

[c] GB2762–2012, accessed through USDA (2014): Pb concerns "fruit products" (p. 4 of the cited document; "fruit products" are further defined as "fruits processed with vinegar, oil and salt," p. 13). Sn concerns "foods" (p. 9 of the cited document).

[d] FRLI (2015): Pb concerns "fruit." Sn concerns "canned food."

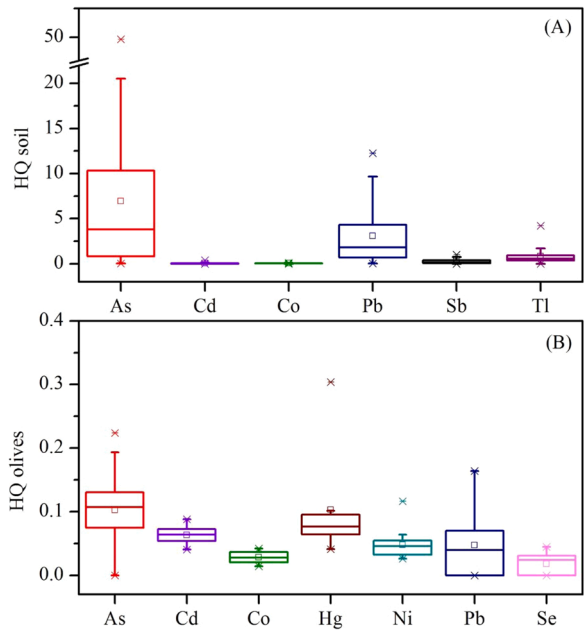

Fig. 4. Hazard quotient (HQ), derived from soil ingestion (A) (35 samples) and table olives consumption (B) (20 samples) of the seven most highly risk-inducing elements in the urban area of Lavrio, southern Greece.

while that of Tl was also very high, but lower than unity (0.83). The HQ of Cd was 0.054, while that of Sb was also low (0.263). The occurrence of such elements as major contributors to health risk is not uncommon in the literature (Nawab et al., 2018). HRA is related not only to the initial PTE soil content, but also to the chronic oral PTE reference dose. For example, As RfD is among the lowest of the measured elements, 1 μg kg^{-1} BW day^{-1}, whereas that of Zn (extremely enriched in soil, but very low in HQ) is as high as 500 μg kg^{-1} BW day^{-1}, a value reflecting that Zn is a major micronutrient. The case of Tl is similar to that of As (RfD = 0.07 μg kg^{-1} BW day^{-1}). The high soil HQ for Tl has rarely been reported in the literature; for example, in a Tl-contaminated area, the HQ of Tl was well below the risk threshold of unity (Liu et al., 2017). Industrial accidents that resulted in the release of high PTE concentrations to soils were not identified as source of significant Tl exposure to health risk (Nadal et al., 2016). Although As is described as a primary source of health risk in the literature, the level of risk reported in our study is rarely observed. For example, Antoniadis et al. (2019b) studied the industrial area of Volos, Greece, while Ding et al. (2018), Huang et al. (2018b), Lin et al. (2018), and Sun and Chen (2018), evaluated highly contaminated areas in China: their results show As HQ values much lower than those found in our study. As for HQ from table olives consumption, values were much lower owing to the lower contents in olive fruits and the relatively low daily consumption rates of 11.23 g per day per capita. However, even in this pathway, As was found to be the element with the highest risk to human health, with a HQ of 0.103, followed by Cd (0.063), Pb (0.048), Ni (0.048), and Hg (0.035).

The average value of the total health risk, HI, was equal to 11.40 for soil ingestion and 0.39 for table olives consumption (Fig. 5). In the soil samples, the HI was above unity in 31 out of the 35 samples, and the maximum value in the study area was 59.62. This extremely high HI is very unusual among similar studies that monitored highly contaminated areas (Reyes et al., 2021; Nguyen et al., 2020). Tang et al. (2017) reported a median HI of 1.40, Li et al. (2015) an HI of 2.45, and Jiang et al. (2017) HI of 3.62, all reporting data from highly contaminated sites. Additionally, Antoniadis et al. (2017b) reported HI as high as 20.81 in a highly contaminated former mining area. Antoniadis et al. (2017c), studied a contaminated area near Athens and reported a mean HI of 1.62. Similarly, Antoniadis et al. (2019b) reported a HI of 3.24 in an

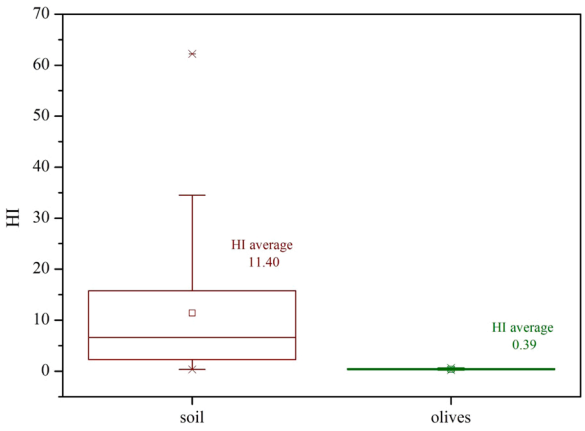

Fig. 5. Hazard index (HI) derived from soil ingestion (35 samples) and table olives consumption (20 samples) induced by all 19 studied elements in the urban area of Lavrio, southern Greece.

industrially contaminated area. For the food-derived HI, we were unable to make comparisons, because, to our knowledge, such information is absent in the literature. However, in studies where both soil and food pathways are assessed, it is often found that soil ingestion produces a higher health risk than that food consumption.

Two elements in our study, As and Pb, listed by USEPA (2016) as those with carcinogenic effects, were used to calculate the carcinogenic risk (CR). In Fig. 6, CR values for both the soil and food are presented separately for each element. CR of lower than 1×10^{-6} is considered acceptable, with the risk increasing when CR values are higher than 1×10^{-4}. A CR value of 10^{-x} denotes a risk of one additional person in a group of 10^{x} persons developing cancer due to this particular exposure. The CR derived from soil As was 31.28×10^{-4}, whereas that from soil Pb was two orders of magnitude lower (91.33×10^{-6}); similarly with the CR related to olive consumption as fruit, the As CR was 1.9×10^{-4} and that of Pb was 14.1×10^{-6}. This shows that As is a major carcinogenic risk factor by either exposure pathways, with each separately producing an unacceptable CR value higher than 1×10^{-4}. This is an unusual finding, especially concerning other studies of contaminated soils in the southeast Mediterranean. Studies based on major Greek cities generated no such potential cancer risk: e.g., Antoniadis et al. (2019b) in Volos, Bourliva et al. (2016) in Thessaloniki, Urrutia-Goyes et al. (2017) in Athens, and Nikolaidis et al. (2013) in northern Greece.

4. Conclusions

The pseudo-total soil concentrations of Ag, As, Cd, Pb, Sb, Tl, and Zn were found in extremely high levels. There is insufficient literature that details similar findings. The XANES spectra revealed that As was predominantly associated with scorodite, Pb with humic substances, while Fe appeared mostly as goethite-like minerals; Zn, was associated with illite in sample #25, with humic substances in sample #29 and also had an evenly distributed association with illite, $Zn(OH)_2$, and humic substances in samples #12 and #18. In table olives, Cd levels surpassed the EU maximum allowable limits in all obtained samples, while Pb surpassed the limits in approximately half of the samples. Hence, we suggest that residents of Lavrio should avoid the consumption of locally produced olives as edible fruits. Health risk assessment confirmed the considerable risk to human health, with As and Pb hazard quotients being well above the risk threshold of HQ = 1. Further research is necessary to develop ecofriendly and feasible remediation plans that should include, apart from the possible introduction of tolerant plant species, soil treatment with suitable additives to achieve hydrogeochemical stabilization, thereby reducing the bioavailability of the highly present PTEs in the study area. Additionally, future research should include other environmental components, such as water to

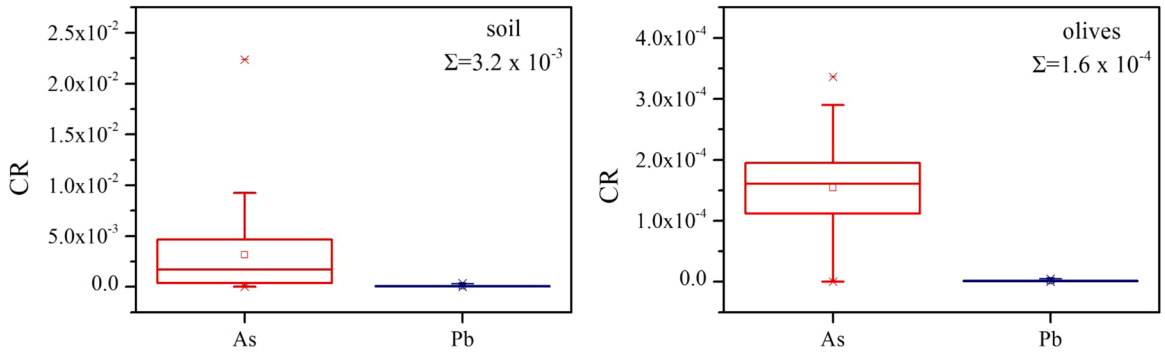

Fig. 6. Cancer risk (CR) derived from soil ingestion (35 samples) and table olives consumption (20 samples) induced by the two carcinogenic elements, As and Pb, in the urban area of Lavrio, southern Greece. The sum of the combined effect of the two elements is denoted as Σ.

further explore the potential health risks.

CRediT authorship contribution statement

Vasileios Antoniadis, Professor: concept, soil and plant sampling, data collection, writing the first draft, embed the corrections of the co-authors, accurateness of calculations, writing, and editing. Giorgos Thalassinos, Doctor: soil and plant sampling, data collection, correction, writing and editing. Efi Levizou, Doctor: Figures, correction, writing and editing. Jianxu Wang, Professor: XANES, correction, writing and editing. Shan-Li Wang, Professor: scientific advice concerning XANES analysis, perform LCF, correction, writing and editing. Sabry M. Shaheen, Professor: writing, correction and editing. Jörg Rinklebe, Professor, supervisor: scientific concept, experimental, laboratory, technical and analytical facilities, supervision, writing, correction and editing.

Declaration of Competing Interest

The authors declare that they have no known competing financial interests or personal relationships that could have appeared to influence the work reported in this paper.

Appendix A. Supporting information

Supplementary data associated with this article can be found in the online version at doi:10.1016/j.jhazmat.2022.128906.

References

Aberg, G., Charalampides, G., Fosse, G., Hjelmseth, H., 2001. The use of Pb isotopes to differentiate between contemporary and ancient sources of pollution in Greece. Atmos. Environ. 35, 4609–4615.

Adewumi, A.J., Laniyan, T.A., Ikhane, P.R., 2020. Distribution, contamination, toxicity, and potential risk assessment of toxic metals in media from Arufu Pb–Zn–F mining area, northeast Nigeria. Toxin Rev. 40, 997–1048. https://doi.org/10.1080/15569543.2020.1815787.

Aide, M., 2009. Three Missouri Alfisols impacted by aeolian deposition of lead-zinc-cadmium-silver-indium bearing mine tailings. Soil Sediment. Contam. 18, 43–54.

Alexakis, D., 2011. Diagnosis of stream sediment quality and assessment of toxic element contamination sources in East Attica, Greece. Environ. Earth Sci. 63, 1689-1383.

Ali, W., Mao, K., Zhang, H., Junaid, M., Xu, N., Rasool, A., Feng, X., Yang, Z., 2020. Comprehensive review of the basic chemical behaviours, sources, processes, and endpoints of trace element contamination in paddy soil-rice systems in rice-growing countries. J. Hazard. Mater. 397, 122720.

Antoniadis, V., Levizou, E., Shaheen, S.M., Ok, Y.S., Sebastian, A., Baum, C., Prasad, M.N. V., Wenzel, W.W., Rinklebe, J., 2017a. Trace elements in the soil-plant interface: phytoavailability, translocation, and phytoremediation—a review. Earth Sci. Rev. 171, 621–645.

Antoniadis, V., Shaheen, S.M., Boersch, J., Frohne, T., Du Laing, G., Rinklebe, J., 2017b. Bioavailability and risk assessment of potentially toxic elements in garden edible vegetables and soils around a highly contaminated former mining area in Germany. J. Environ. Manag. 186, 192–200.

Antoniadis, V., Golia, E.E., Shaheen, S.M., Rinklebe, J., 2017c. Bioavailability and health risk assessment of potentially toxic elements in Thriasio Plain, near Athens, Greece. Environ. Geochem. Health 39, 319–330.

Antoniadis, V., Shaheen, S.M., Levizou, E., Shahid, M., Niazi, N.B., Vithanage, M., Ok, Y. S., Bolan, N., Rinklebe, J., 2019a. A critical prospective analysis of the potential toxicity of trace element regulation limits in soils worldwide: are they protective concerning health risk assessment?—a review. Environ. Int. 127, 819–847.

Antoniadis, V., Golia, E.E., Liu, W.-T., Wang, S.-L., Shaheen, S.M., Rinklebe, J., 2019b. Soil and maize contamination by trace elements and associated health risk assessment the industrial area of Volos, Greece. Environ. Int. 124, 79–88.

Athena, User's Manual, 2005. 2D Process Simulation Software. Silvaco International, Version 5.10.0.R., Santa Clara, USA.

Bargagli, R., 1995. The elemental composition of vegetation and the possible incidence of soil contamination of samples. Sci. Total Environ. 176, 121–128.

Bluteau, M.-C., Demorpoulos, G.P., 2007. The incongruent dissolution of scorodite—solubility, kinetics and mechanism. Hydrometallurgy 87, 163–177.

Bourliva, A., Papadopoulou, L., Aidona, E., 2016. Study of road dust magnetic phases as the main carrier of potentially harmful trace elements. Sci. Total Environ. 553, 380–391.

CEC (Council of the European Communities), 1986. The Protection of the Environment, and in Particular of the Soil, When Sewage Sludge is Used in Agriculture. Council Directive of 12 June 1986. Official Journal of the European Communities No L 181/6.

CEC (Commission of the European Communities), 2006. Commission Regulation (EC) No 1881/2006 of 19 December 2006 "Setting Maximum Levels for Certain Contaminants in Foodstuffs." Official Journal of the European Communities.

CEC (Commission of the European Communities), 2008. Commission Regulation (EC) No 629/2008 of 2 July 2008, Amending Regulation (EC) No 1881/2006 "Setting Maximum Levels for Certain Contaminants in Foodstuffs." Official Journal of the European Communities.

Ding, Z., Li, Y., Sun, Q., Zhang, H., 2018. Trace elements in soils and selected agricultural plants in the Tongling mining area of China. Int. J. Environ. Res. Public Health 15, 202.

FAO/WHO (Food and Agriculture Organization/World Health Organization), 2017. Codex Alimentarius Commission—International Food Standards. General Standard for Contaminants Toxins in Food and Feed CXS 193–1995. Available at ⟨www.fao.org/input/download/standards/17/CXS_193e_2015.pdf⟩ (Last access on 15 January 2022).

FAO, 2020. Table Olive Market. ⟨https://www.fao.org/3/y4890e/y4890e0h.htm⟩ (Accessed 14 January 2022).

FRLI (Federal Register of Legislative Instruments), 2015. Standard 1.4.1. Contaminants and Natural Toxicants. Issue 124, 15 January 2015. (Available at ⟨https://www.legislation.gov.au/Details/F2015C00052⟩; last (Accessed 15 January 2022).

Fourati, R., Scopa, A., Ahmed, C.B., Abdallah, F.B., Terzano, R., Gattullo, C.E., Allegretta, I., Galgano, F., Caruso, M.C., Sofo, A., 2017. Leaf biochemical responses and fruit oil quality parameters in olive plants subjected to airborne metal pollution. Chemosphere 168, 514–522.

Funes Pinter, I., Salomon, M.V., Gil, R., Mastrantonio, L., Bottini, R., Piccoli, P., 2018. Arsenic and trace elements in soil, water, grapevine and onion in Jachal, Argentina. Sci. Total Environ. 615, 1485–1498.

Gabersek, M., Gosar, M., 2018. Geochemistry of urban soil in the industrial town of Maribor, Slovenia. J. Geochem. Explr. 187, 141–154.

Gabersek, M., Gosar, M., 2021. Towards a holistic approach to the geochemistry of solid inorganic particles in the urban environment. Sci. Total Environ. 763, 144214.

Gallero, J.L.R., Ortiz, J.E., Sanchez-Palencia, Y., Baragano, D., Borrego, A.G., Torres, T., 2019. A multivariate examination of the timing and accumulation of potentially toxic elements at Las Conchas bog (NW Spain). Environ. Pollut. 254, 113048.

Gurel, S., Basar, H., 2014. Metal status of olive trees grown in southeastern Marmara region of Turkey. Commun. Soil Sci. Plant Anal. 45, 1464–1479.

Hadjipanagiotou, C., Christou, A., Zissimos, A.M., Chatzitheodoridis, E., Varnavas, S.P., 2020. Contamination of stream waters, sediments, and agricultural soil in the surroundings of an abandoned copper mine by potentially toxic elements and associated environmental and potential human health-derived risks: A case study from Agrokipia, Cyprus. Environ. Sci. Pollut. Res. 27, 41279–41298.

Hou, D., O'Connor, D., Igalavithana, A.D., Alessi, D.S., Luo, J., Tsang, D.C.W., Sparks, D. L., Yamauchi, Y., Rinklebe, J., Ok, Y.S., 2020. Metal contamination and bioremediation of agricultural soils for food safety and sustainability. Nat. Rev. Earth Environ. 1, 366–381.

Huang, X., Li, N., Wu, Q., Long, J., Luo, D., Huang, X., Li, D., Zhao, D., 2018a. Fractional distribution of thallium in paddy soil and its bioavailability to rice. Ecotoxicol. Environ. Saf. 148, 311–317.
Huang, Y., Chen, Q., Deng, M., Japenga, J., Li, T., Yang, X., He, Z., 2018b. Heavy metal pollution and health risk assessment of agricultural soils in a typical peri-urban area in southeast China. J. Environ. Manag. 207, 159–168.
Huang, Y.-N., Dang, F., Li, M., Zhou, D.-M., Song, Y., Wang, J.-B., 2020. Environmental and human health risks from metal exposures nearby a Pb-Zn-Ag mine, China. Sci. Total Environ. 698, 134326.
Jiang, Y., Chao, S., Liu, J., Yang, Y., Chen, Y., Zhang, A., Cao, H., 2017. Source apportionment and health risk assessment of heavy metals in soil for a township in Jiangsu Province, China. Chemosphere 168, 1658–1668.
Jones, J., Wolf, J.B., Mills, H.A., 1991. Plant Analysis Handbook: A Practical Sampling, Preparation, Analysis, and Interpretation Guide. Athens, USA.
Jung, M.C., 2001. Heavy metal contamination of soils and waters in and around the Imcheon Au-Ag mine, Korea. Appl. Geochem. 16, 1369–1375.
Kabata-Pendias, A., 2011. Trace Elements in Soils and Plants, Fourth ed.,. CRC Press, Boca Raton.
Kalyvas, G., Gasparatos, D., Papassiopi, N., Massas, I., 2018. Topsoil pollution as ecological footprint of historical mining activities in Greece. Land Degrad. Dev. 29, 2025–2035.
Korre, A., Durucan, S., Koutroumani, A., 2002. Quantitative-spatial assessment of the risks associated with high Pb loads in soils around Lavrio, Greece. Appl. Geochem. 17, 1029–1045.
Langmuir, D., Mahoney, J., Rowson, J., 2006. Solubility products of amorphous ferric arsenate and crystalline scorodite ($FeAsO_4{\cdot}2H_2O$) and their application to arsenic behavior in buried mine tailings. Geochem. Cosmochim. Acta 70, 2942–2956.
Lee, C.G., Chon, H.-T., Jung, M.C., 2001. Heavy metal contamination in the vicinity of the Daduk Au-Ag-Pb-Zn mine in Korea. Appl. Geochem. 16, 1377–1386.
Lewinska, K., Karczewska, A., 2019. Antimony in soils of SW Poland—an overview of potentially enriched sites. Environ. Monit. Assess. 191, 70.
Li, P., Lin, C., Cheng, H., Duan, X., Lei, K., 2015. Contamination and health risks of soil heavy metals around a lead/zinc smelter in southwestern China. Ecotoxicol. Environ. Saf. 113, 391–399.
Lin, M., Li, S., Sun, X., Yang, S., Li, J., 2018. Heavy metal contamination in green space soils of Beijing, China. Acta Agric. Scand. B Soil Plant Sci. 68, 291–300.
Liu, J., Luo, X., Wang, J., Xiao, T., Chen, D., Sheng, G., Yin, M., Lippold, H., Wang, C., Chen, Y., 2017. Thallium contamination in arable soils and vegetables around a steel plant—a newly-found significant source of Tl pollution in South China. Environ. Pollut. 224, 445–453.
Liu, Q., Li, H., Jin, G., Zheng, K., Wang, L., 2018. Assessing the influence of humic acids on the weathering of galena and its environmental implications. Ecotoxicol. Environ. Saf. 158, 230–238.
Liu, Y., Fei, X., Zhang, Z., Li, Y., Tang, J., Xiao, R., 2020. Identifying the sources and spatial patterns of potentially toxic trace elements (PTEs) in Shanghai suburb soils using global and local regression models. Environ. Pollut. 264, 114171.
Luo, X., Ren, B., Hursthouse, A.S., Jiang, F., Deng, R.-J., 2020. Potentially toxic elements (PTEs) in crop, soil, and water near Xiangtan manganese mine, China: Potential risk to health in the foodchain. In: Environ. Geochem. Health, 42, pp. 1965–1976.
Majzlan, J., Drahota, P., Filippi, M., 2014. Parageneses and crystal chemistry of arsenic minerals. In: Bowell, R.J., Alpers, C.N., Jamieson, H.E., Nordstrom, D.K., Majzlan, J. (Eds.), Arsenic: Environmental Geochemistry, Mineralogy, and Microbiology Reviews in Mineralogy & Geochemistry. Mineralogical Society of America, Chantilly, VA, pp. 17–184.
Mariet, A.-L., de Vaufleury, A., Begeot, C., Walter-Simonnet, A.-V., Gimbert, F., 2016. Palaeo-pollution from mining activities in the Vosges Mountains: 1000 years and still bioavailable. Environ. Pollut. 214, 575–584.
Mbadugha, L., Cowper, D., Dossanov, S., Paton, G.I., 2020. Geogenic and anthropogenic interactions at a former Sb mine: environmental impacts of As and Sb. Environ. Geochem. Health 42, 3911–3924.
Mora, A., Jumbo-Flores, D., Gonzalez-Merizalde, M., Bermeo-Flores, S.A., Alvarez-Figueroa, P., Mahlknecht, J., Hernandez-Antonio, A., 2019. Heavy metal enrichment factors in fluvial sediments of an Amazonian basin impacted by gold mining. Bull. Environ. Contam. Toxicol. 102, 210–217.
Mykolenko, S., Liedienov, D., Kharytonov, M., Makieieva, N., Kuliush, T., Queralt, I., Margui, E., Hidalco, M., Pardini, G., Gispert, M., 2018. Presence, mobility and bioavailability of toxic metal(loid)s in soil, vegetation and water around a Pb-Sb recycling factory (Barcelona, Spain). Environ. Pollut. 237, 569–580.
Nadal, M., Rovira, J., Diaz-Ferrero, J., Schuchmacher, M., Domingo, J.L., 2016. Human exposure to environmental pollutants after a tire landfill fire in Spain: Health risks. Environ. Int. 97, 37–44.
Nawab, J., Farooqi, S., Xiaoping, W., Khan, S., Khan, A., 2018. Levels, dietary intake, and health risk of potentially toxic metals in vegetables, fruits, and cereal crops in Pakistan. Environ. Sci. Pollut. Res. 25, 5558–5571.
Nguyen, T.H., Hoang, H.N.T., Bien, N.Q., Tuyen, L.H., Kim, K.-W., 2020. Contamination of heavy metals in paddy soil in the vicinity of Nui Phao multi-metal mine, North Vietnam. Environ. Geochem. Health 42, 4141–4158.
Nikolaidis, C., Orfanidis, M., Hauri, D., Mylonas, S., Constantinidis, T., 2013. Public health risk assessment associated with heavy metal and arsenic exposure near an abandoned mine (Kirki, Greece). Int. J. Environ. Health Res. 23, 507–519.
Oyarzun, R., Lillo, J., Lopez-Garcia, J.A., Esbri, J.M., Cubas, P., Llanos, W., Higueras, P., 2011. The Mazarron Pb-(Ag)-Zn mining district (SE Spain) as a source of heavy metal contamination in a semiarid realm: Geochemical data from mine wastes, soils, and stream sediments. J. Geochem. Explor. 109, 113–124.
Palansooriya, K.N., Shaheen, S.M., Tsang, S.C.D.C.W., Hashimoto, Y., Hou, D., Bolan, N., Rinklebe, J., Ok, Y.S., 2020. Soil amendments for immobilization of potentially toxic elements in contaminated soils: a critical review. Environ. Int. 134, 105046.
Panagopoulos, I., Karayiannis, A., Adam, K., Aravossis, K., 2009. Application of risk management techniques for the remediation of an old mining site in Greece. Waste Manag. 29, 1739–1746.
Pappa, F.K., Tsabaris, C., Patiris, D.L., Androulakaki, E.G., Eleftheriou, G., Betsou, C., Michalopoulou, V., Kokkoris, M., Vlastou, R., 2018. Historical trends and assessment of radionuclides and heavy metals in sediments near an abandoned mine, Lavrio, Greece. Environ. Sci. Pollut. Res. 25, 30084–30100.
Pavlovic, P., Savvidis, T., Breuste, J., Kostic, O, Cakmak, D., Dordevic, D., Pavlovic, D., Pavlovic, M., Perovic, V., Mitrovic, M., 2021. Fractionation of potentially toxic elements (PTEs) in urban soils from Salzburg, Thessaloniki and Belgrade: An insight into source identification and human health risk assessment. Int. J. Environ. Res. Public Health 18, 6014.
Petousi, I., Fountoulakis, M.S., Saru, M.L., Nikolaidis, N., Fletcher, L., Stentiford, E.I., Manios, T., 2015. Effects of reclaimed wastewater irrigation on olive (*Olea europea* L. cv. 'Koroneiki') trees. Agr. Water Manag. 160, 33–40.
Ravel, B., Newville, M., 2005a. ATHENA and ARTEMIS: Interactive graphical data analysis using IFEFFIT. Phys. Scr. T115, 1007–1010.
Ravel, B., Newville, M., 2005b. ATHENA, ARTEMIS, HEPHAESTUS: data analysis for X-ray absorption spectroscopy using IFEFFIT. J. Synchrotron Radiat. 12, 537–541.
Reyes, A., Cuevas, J., Fuentes, B., Fernandez, E., Arce, W., Guerrero, M., Letelier, M.V., 2021. Distribution of potentially toxic elements in soils surrounding abandoned mining waste located in Taltal, Northern Chile. J. Geochem. Explor. 220, 106653.
Rinklebe, J., Antoniadis, V., Shaheen, S.M., Rosche, O., Altermann, M., 2019. Health risk assessment of potentially toxic element with the aid of indices on the example of soils along the Central Elbe River as a model region. Environ. Int. 126, 76–88.
Rodriguez-Iruretagoiena, A., de Vallajuelo, S.F.-O., de Diego, A., de Leao, F.B., de Medeiros, D., Oliveira, M.L.S., Tafarel, S.R., Arana, G., Madariaga, J.M., Silva, L.F.O., 2016. The mobilization of hazardous elements after a tropical storm event in a polluted estuary. Sci. Total Environ. 565, 721–729.
Rowell, D.L., 1994. Soil Science: Methods and Applications. Prentice Hall, Harlow, UK.
Schwab, A.P., Lindsay, W.L., Smith, P.J., 1983. Elemental contents of plants growing on soil-covered retorted shale. J. Environ. Qual. 12, 301–304.
Shaheen, S.M., Antoniadis, V., Kwon, E., Song, H., Wanexplg, S.-L., Hseu, Z.-Y., Rinklebe, J., 2020. Soil contamination by potential toxic elements and the associated human health risk in geo- and anthropogenic contaminated soils: a case study from the temperate region (Germany) and the arid region (Egypt). Environ. Pollut. 262, 114312.
Shahmoradi, B., Hajimirzaei, S., Amanollahi, J., Wantalla, K., Maleki, A., Lee, S.-M., Shim, M.J., 2020. Influence of iron mining activity on heavy metal contamination in the sediments of the Aqyazi River, Iran. Environ. Monit. Assess. 192, 521.
Sofianska, E., Michailidis, K., 2016. Assessment of heavy metals contamination and potential ecological risk in soils affected by a former Mn mining activity, Drama District, Northern Greece. Soil Sediment Contam. 25, 296–312.
Soltanpour, P.N., Schwab, A.P., 1977. A new soil test for simultaneous extraction of macro- and micro-nutrients in alkaline soils. Commun. Soil Sci. Plant Anal. 8, 195–207.
Stamatis, G., Voudouris, K., Karefilakis, F., 2001. Groundwater pollution by heavy metals in historical mining area of Lavrio, Attica, Greece. Water Air Soil Pollut. 128, 61–83.
Sun, Z., Chen, J., 2018. Risk assessment of potentially toxic elements (PTEs) pollution at a rural industrial wasteland in an abandoned metallurgy factory in North China. Int. J. Environ. Res. Public Health 15, 85.
Tang, Z., Chai, M., Cheng, J., Jin, J., Yang, Y., Nie, Z., Huang, Q., Li, Y., 2017. Contamination and health risks of heavy metals in street dust from a coal-mining city in Eastern China. Ecotoxicol. Environ. Saf. 138, 83–91.
Tang, Z., Deng, R.-J., Zhang, J., Ren, B.-Z., Hursthouse, A., 2020. Regional distribution characteristics and ecological risk assessment of heavy metal pollution of different land use in an antimony mining area—Xikuangshan. China Hum. Ecol. Risk Assess. 26, 1779–1794.
Teng, F., Zhang, Y., Wang, D., Shen, M., Hu, D., 2020. Iron-modified rice husk hydrochar and its immobilization affect for Pb and Sb in contaminated soil. J. Hazard. Mater. 398, 122977.
Tsadila, E., Tsadilas, C., Stamatiadis, S., Christodoulakis, N., 2009. Investigation of soil property changes and olive tree stress as caused by excessive sewage sludge application. Commun. Soil Sci. Plant Anal. 40, 514–525.
Tuna, B., Gecgel, U., 2011. Determination of heavy metals and micronutrients in olives grown under different conditions. Fresenius Environ. Bull. 20, 2883–2889.
Urrutia-Goyes, R., Argyraki, A., Ornelas-Soto, N., 2017. Assessing lead, nickel, and zinc pollution in topsoil from a historic shooting range rehabilitated into a public urban park. Int. J. Environ. Res. Public Health 14, 698.
USEPA (United States Environment Protection Agency), 2002. OSWER 9355.4–24 December 2002. Supplemental Guidance for Developing Soil Screening Levels for Superfund Sites. Office of Emergency and Remedial Response, U.S. Environmental Protection Agency, Washington, DC 20460. Available at https://nepis.epa.gov/Exe/ZyNET.exe/91003IJK.TXT?ZyActionD=ZyDocument&Client=EPA&Index=2000+Thru+2005&Docs=&Query=&Time=&EndTime=&SearchMethod=1&TocRestrict=n&Toc=&TocEntry=&QField=&QFieldYear=&QFieldMonth=&QFieldDay=&IntQFieldOp=0&ExtQFieldOp=0&XmlQuery=&File=D%3A%5Czyfiles%5CIndex%20Dat%5C00thru05%5CTxt%5C00000023%5C91003IJK.txt&User=ANONYMOUS&Password=anonymous&SortMethod=h%7C-&MaximumDocuments=1&FuzzyDegree=0&ImageQuality=r75g8/r75g8/x150y150g16/i425&Display=hpfr&DefSeekPage=x&SearchBack=ZyActionL&Back=ZyActionS&BackDesc=Results%

20page&MaximumPages=1&ZyEntry=1&SeekPage=x&ZyPURL (Last Accessed 15 January 2022).

USEPA (United States Environment Protection Agency), 2016. Regional Screening Levels (RSLs) - Generic Tables (May 2016) (TR=1E-06 THQ=0.1). Available at http://www.sviva.gov.il/subjectsenv/contaminatedsoil/documents/epa%20regional%20screening%20levels%20(rsl)%20summary%20table,%20nov%202015.pdf (Last Accessed 15 January 2022).

USEPA (United States Environment Protection Agency), 2017. National Primary Drinking Water Regulations. Available at https://www.epa.gov/ground-water-and-drinking-water/national-primary-drinking-water-regulations (Last Accessed 15 January 2022).

USDA (United Sates Department of Agriculture), 2014. China's Maximum Levels for Contaminants in Foods. Foreign Agricultural Service, Global Agricultural Information Network, Report #14058 concerning National Food Safety Standard of Maximum Levels of Contaminants in Foods (GB 2762–2012). Available at https://gain.fas.usda.gov/Recent%20GAIN%20Publications/Maximum%20Levels%20of%20Contaminants%20in%20Foods%20_Beijing_China%20-%20Peoples%20Republic%20of_12–11-2014.pdf (Last Accessed 15 January 2022).

Wang, S., Zheng, K., Liu, Q., Wang, L., Feng, X., Li, H., 2021. Galena weathering in simulated alkaline soil: lead transformation and environmental implications. Sci. Total Environ. 755, 142708.

Xi, X., Liu, Y., Qiu, H., Yang, X., 2020. Quantifying ecological health risks of heavy metals from different sources in farmland soils within a typical mining and smelting industrial area. Environ. Geochem. Health. https://doi.org/10.1007/s10653-020-00731-y.

Xiao, T., Guha, J., Boyle, D., Liu, C.-Q., Zheng, B., Wilson, G.C., Rouleau, A., Chen, J., 2004a. Naturally occurring thallium: a hidden geoenvironmental health hazard? Environ. Int. 40, 501–507.

Xiao, T., Guha, J., Boyle, D., Liu, C.-Q., Chen, J., 2004b. Environmental concerns related to high thallium levels in soils and thallium uptake by plants in southwest Guizhou, China. Sci. Total Environ. 318, 223–244.

Yang, P.T., Wu, W.J., Hashimoto, Y., Huang, J.H., Huang, S.T., Hseu, Z.Y., Wang, S.L., 2020. Evolution of As speciation with depth in a soil profile with a geothermal As origin. Chemosphere 241, 124956.

Yildirim, D., Sasmaz, A., 2017. Phytoremediation of As, Ag, and Pb in contaminated soils using terrestrial plants grown on Gumuskoy mining area (Kutahya Turkey). J. Geochem. Explor. 182, 228–234.

Zaanouni, N., Gharssallaoui, M., Eloussaief, M., Gabsi, S., 2018. Heavy metals transfer in the olive tree and assessment of food contamination risk. Environ. Sci. Pollut. Res. 25, 18320–18331.

Zhang, Z., Zhang, N., Li, H., Lu, Y., Wang, Q., Yang, Z., 2019. Risk assessment, spatial distribution, and source identification of heavy metal(loid)s in paddy soils along the Zijiang River basin, in Hunan Province, China. J. Soil. Sediment. 19, 4042–4051.

Zhou, Y., Wang, L., Xiao, T., Chen, Y., Beiyuan, J., She, J., Zhou, Y., Yin, M., Liu, J., Liu, Y., Wang, Y., Wang, J., 2020. Legacy of multiple metal(loid)s contamination and ecological risks in farmland soils from a historical artisanal zinc smelting area. Sci. Total Environ. 720, 137541.